TR-IIS-05-004

Queuing Delay Propagation Model (QDPM)-based Queuing Region Determination for Available Bandwidth Estimation of Multimedia QoS

Yu-Chen Huang, Chun-Shien Lu, Hsiao-Kuang Wu

Queuing Delay Propagation Model (QDPM)-based

Queuing Region Determination for

Available Bandwidth Estimation of Multimedia QoS

Yu-Chen Huang[1,2], Chun-Shien Lu[1,*], Hsiao-Kuang Wu[2]

[1]Institute of Information Science, Academia Sinica, Taipei, Taiwan, ROC

[2]Dept. Computer Sci. & Information Eng., National Central Uni., Chung-Li, Taiwan, ROC

Abstract

Available bandwidth is an important factor that can be used to adapt the sending rate to network conditions, so that packet loss, caused by congestion, can be significantly reduced before error control mechanisms are employed. To this end, we propose an active probing-based queuing delay propagation model (QDPM)-based scheme for available bandwidth estimation. Common assumptions, including use of the fluid traffic model and restriction to the single-hop network model, that have been made in the literature are relaxed in this study. Unlike the increasing trend of one-way delays that is widely used in probe rate model-based methods, in the proposed method, we exploit the magnitude relationship among the input gap, output gap, and queuing delay to define the types of queuing regions for each packet pair. In addition, we quantify the captured traffic ratio (CTR), which is defined as the total output gaps of joint queuing regions per total input gaps, and use it to derive the relationship between probing rate and available bandwidth. To justify the performance of our method, we further investigate how the estimation resolution and the probing noise ratio are related to the accuracy of available bandwidth estimation. Extensive simulations have been conducted and comparisons with other methods have been made to verify the effectiveness of our method for accurate and smooth estimation, no matter whether single-hop or multi-hop environments are considered.

keywords: Available bandwidth, Bottleneck, Congestion, Quality-of-Service (QoS), Queuing delay, Queuing region, TCP

I. INTRODUCTION

A. Background

For multimedia transmission over a network, bandwidth is a key factor that affects the packet loss rate, which may be severe if the sending rate is not adaptively adjusted according to the network conditions. In order to exploit network bandwidth efficiently, multimedia data (e.g., video) needs to be compressed in advance before transmission. However, when packet loss occurs, reference errors that occur during decoding will be propagated, further degrading the quality of the decoded data. In order to enable decoded video to be displayed with uniform quality, the network needs to provide quality-of-service (QoS) [24] for multimedia transmission. In this paper, we shall focus on available bandwidth estimation, which is closely related to congestion control and adaptive rate adjustment.

In the literature, numerous approaches have been presented for estimating network bandwidth. In [1], Dutta and Zhang improved the current Internet infrastructure so as to support different kinds of QoS in core networks. However, their method undesirably changes the intermediate nodes of a network; thus, scalability is lost. In [11], [12], [19], [24], methods were proposed for adjusting the transmission rate according to the current network conditions. Their common characteristic is that a scalable video coding scheme is incorporated with a network behavior monitor. The key to these solutions lies in how to reliably detect network conditions, where congestion plays a crucial role. When the propagation path is congested (which means the arrival rate of aggregated traffic† is higher than the maximum service rate of the bottleneck router), incoming packets will be queued in the router. Once the queue overflows, packets start to be dropped, and the sender needs to wait for a time out to retransmit the dropped packets. In addition, excessive delay will cause the receiver to drop the delayed packets, resulting in packet loss. Traditional transport protocols (e.g., TCP) are still insufficient for dealing with congestion because they rely on an indication of packet loss to adjust the sending rate in a blind manner such that video transmissions with stable quality cannot be guaranteed. For this reason, the protocol UDP and an additional congestion control mechanism are usually combined to facilitate video transmission.

In order to deal with congestion, we prefer to handle control the sending rate through available bandwidth estimation. The idea behind our method is that bandwidth utilization and variation are closely related to the sending rate, congestion, and packet loss. Our idea is also supported by the fact that (1) aggregated TCP throughput is stationary and the individual TCP rate varies less than a factor of hours [25]; and (2) that intermediate nodes on the Internet are often stable, and the routing paths of flows remain unchanged for a long period of hours or days

---

†Here, aggregated traffic is composed of probing traffic and cross traffic.

[18]. The above facts indicate that available bandwidth estimation can be used to predict the future behavior of a propagation path over the Internet. In addition, available bandwidth can be used to improve the performance of a network. For example, Hu and Steenkiste proposed using *PaSt* [3] to set the slow-start threshold based on active estimation of the available bandwidth so that the bandwidth can be sufficiently utilized, while Ribeiro *et al.* [22] proposed locating available bandwidth bottlenecks through available bandwidth estimation.

Active probing has been found to be useful for discovering network conditions. In [10], Keshav proposed a new idea, called the "packet pair," to estimate the capacity of a bottleneck link, which is defined as the minimum capacity among the links from the sender to the receiver. However, the capacity of a bottleneck link is not really important enough to affect network conditions. On the contrary, available bandwidth has been recognized as the most important factor. In [7], available bandwidth was determined from all the links as the minimum bandwidth that has not been used. Thus, it is known that a bottleneck link is not necessarily the link with the minimum available bandwidth.

In order to actively estimate available bandwidth, packet trains are sent and interact with cross traffic such that a "turning point" is generated to reveal the relationship between the cross traffic rate and probing rate. Specifically, a turning point represents a "transition," where the probing rate is equal to the available bandwidth. Under this circumstance, the bottleneck router will be busy handling incoming traffic, including cross and probing traffic. Although active probing-based bandwidth estimation has become a hot topic [5] recently, some may wonder whether any available bandwidth will still remain after TCP bulk transfer. In fact, if bulk transfer drains all the bandwidth, then all the TCP flows will go back to the congestion avoidance phase. Under this circumstance, available bandwidth will appear after the network becomes stationary. The same observation can also be found in [7]. As a result, available bandwidth indeed exists in networks and plays a crucial role in revealing network conditions [2], [4], [8], [13], [15], [17], [20], [21], [23].

B. Our Contributions

Our main contribution is that the common assumptions, including the restriction to a single-hop network model only and use of the fluid traffic model, that have been made in the literature are relaxed. We will present a strategy called the "queuing delay propagation model (QDPM)" that can be used to determine the type of a queuing region that exists within a packet pair, and we will investigate the key factors affecting the determination. Here, the queuing region is divided into two parts: the joint queuing region (JQR) and disjoint queuing region (DQR). The proposed method also defines the "captured traffic ratio (CTR)," which is the ratio of the total output gaps accumulated

from JQRs per total input gaps and is used to determine the relationship between the probing rate and available bandwidth. Most importantly, our idea can be merged with the existing (either PGM or PRM) methods to further improve their inherent disadvantages, as summarized in Table. I.

TABLE I

COMPARISON AMONG DIFFERENT TYPES OF AVAILABLE BANDWIDTH ESTIMATION METHODS

Methods	Single-hop only	Fluid cross traffic only
PGM [2], [17], [20], [23]	Yes	Yes
PRM [4], [8], [13], [15], [21]	No	Yes
QDPM	No	No

The remainder of this paper is organized as follows. Related work is presented in Sec. II. In Sec. III, we propose a so-called "queuing delay propagation model (QDPM)" to precisely determine the types of queuing regions for each packet pair. Then, the so-called "captured traffic ratio" is proposed to indicate the relationship between the probing rate and available bandwidth. In Sec. IV, the issues concerning the estimation resolution and probing noise ratio that are relevant to the proposed method are discussed. In Sec. V, simulation results are given and comparisons with other methods are made to demonstrate the excellent performance of our method. Finally, concluding remarks are made in Sec. VI.

II. RELATED WORKS

The existing active probing-based available bandwidth estimation technologies can be roughly divided into two categories [23]: (1) probe gap model (PGM) methods; and (2) probe rate model (PRM) methods. Some representative approaches including Pathload, Pathbw, and IGI, which have been reviewed and their characteristics and weaknesses pointed out.

A. Probe Rate Model (PRM)-based Methods

The idea behind PRM methods [4], [8], [13], [15], [21] is to exploit self-induced congestion, which relies on an intuitive assumption that if the probing rate is higher than the available bandwidth, then the probing packets will start to be queued in the bottleneck router, resulting in increased queuing delays. More specifically, one-way delays are determined by three factors: service, queuing, and transmission delays. Let the propagation path be composed of H links, and let each hop, hop_h ($1 \leq h \leq H$), consist of a FIFO queue and a store and forward router. The

one-way delay of the i-th packet P^i, OWD^i, at a single hop h is

$$OWD^i = \tau^i - \tau^i_* = D^i + x^i + t^i, \tag{1}$$

where τ^i_* denotes the departure time of P^i sent from the sender, τ^i denotes the arrival time of P^i received at the receiver, D^i denotes the queuing delay, x^i denotes the service delay, and t^i denotes the transmission delay. Based on Eq. (1), the OWD jitter, ΔOWD^i, measured as the difference between two one-way delays, can be expressed as

$$\Delta OWD^i \quad = OWD^i - OWD^{i-1} =$$
$$(t^i - t^{i-1}) \quad + (x^i - x^{i-1}) + (D^i - D^{i-1}), \tag{2}$$

which can be further simplified as

$$\Delta OWD^i = D^i - D^{i-1}, \tag{3}$$

based on the conditions that the difference between transmission delays can be eliminated if the packets are transferred over the same path, and that the difference between service delays can be eliminated if the packet size is the same.

Similarly, when a multi-hop environment is considered, the OWD jitter of a path can be obtained by summing the OWD jitters (Eq. (3)) of all the hops for the ith packet pair as follows:

$$\Delta OWD^i = \sum_{h=1}^{H} (D^i_h - D^{i-1}_h). \tag{4}$$

In [8], Jain and Dovrolis pointed out that the queuing delay of probing packets is dominated by the delay caused by the tight-link, i.e.,

$$\Delta OWD^i = D^i_{tl} - D^{i-1}_{tl}, \tag{5}$$

where tl ($\in [1 \ H]$) denotes the location of the tight link and $D^i_h - D^{i-1}_h = 0$ holds for $h \neq tl$. The OWD jitters in Eq. (5) can result in two trends: OWD increasing trend if most the ΔOWD^i's are larger than zero and OWD decreasing trend if most the ΔOWD^i's are smaller than zero. Although OWD decreasing trend was previously regarded as useless for estimating available bandwidth, we find in this study that it indeed provides useful information (as will be explained in Sec. III-A.3.a).

The probability of OWD increasing trend as adopted in [13] is determined by comparing[‡] two OWDs in a single hop as follows:

$$Prob\{OWD^l > OWD^m\} > 0.5, \ \forall \ l > m. \tag{6}$$

[‡]In [8], a different type of comparison was adopted.

Eq. (6) implies that if the probability of an increasing OWD ratio is larger than 0.5, then increasing OWD will occur in an OWD sequence. However, this level of accuracy depends on the characteristic of the cross traffic model. If the cross traffic operates like a fluid traffic model [9], then the variation of the arrival rates will tend to be smooth. Under this circumstance, the amount of cross traffic inserted between each packet pair should be approximately the same, and the queuing delay will be an increasing and smoothing sequence if the probing rate is higher than the available bandwidth. Unfortunately, TCP is bursty instead of fluid, so OWD increasing trend does not suffice to represent the relationship between the probing rate and available bandwidth, especially, when the cross traffic rate varies during measurement. A scenario is depicted in Fig. 1, where one-way delay increasing trend is not detected even when the probing rate is higher than the available bandwidth.

On the other hand, the computational complexity of calculating OWD increasing trend, as indicated in Eq. (6), is $O(P_{length}^2)$, where P_{length} is the number of packet pairs in a packet train. This higher complexity is an obstacle to adopting longer packet trains. In addition, the use of longer packet trains also implies that the estimated results will tend to be outdated, and that much computational power will be needed in a wireless environment.
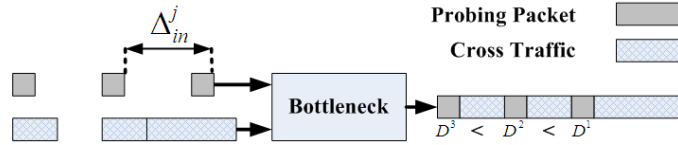

Fig. 1. An error in PRM, where the probing rate Δ_{in}^j of the j-th packet train is higher than the available bandwidth, and the cross traffic rate decreases progressively during measurement. "D^i" denotes the queuing delay of the i-th probing packet. The one-way delay increasing trend is not detected to wrongly determine that the probing rate is smaller than the available bandwidth.

B. Probe Gate Model (PGM)-based Methods

In PGM-based methods [2], [17], [20], [23], probing packets are sent into the network in the hope that they can be expanded by cross traffic when the probing rate is higher than the available bandwidth. Under this circumstance, if the size of the cross traffic placed in between the packet pair can be known, then it is possible to directly estimate the available bandwidth as the bottleneck link capacity minus the cross traffic rate. Two assumptions are made in PGM so that reliable and fast available bandwidth estimation can be better guaranteed without the need to pour many probing trains to the network. These two assumptions are as follows: (1) a single-hop environment is assumed such that the link with the minimum available bandwidth is the same as the bottleneck link; (2) the packet train must operate in joint queuing regions due to the use of a fluid cross traffic model. Unlike PRM, PGM focuses on directly inferring the cross traffic rate from the packet pairs instead of the OWD increasing trend in a packet train.

Let us take IGI [2] an example to illustrate how a PGM-based method works. Basically, IGI involves two tasks: determining the turning point and estimating the cross traffic rate. The turning point is determined to check whether a packet train is operating in a joint queuing region (JQR), defined as follows:

A packet train is operating in a JQR if

$$\frac{|\sum_{i=1}^{P_{length}} \Delta_{out}^i - \sum_{i=1}^{P_{length}} \Delta_{in}^j|}{max(\sum_{i=1}^{P_{length}} \Delta_{out}^i, \sum_{i=1}^{P_{length}} \Delta_{in}^j)} > \delta, \tag{7}$$

where Δ_{in}^j denotes the inter-departure time (or input probing gap) of the j-th packet train at the sender, Δ_{out}^i denotes the inter-arrival time (or output probing gap) of the i-th packet pair arriving at the receiver, and δ is the threshold used to determine the existence of a turning point. In [2], Hu and Steenkiste suggested that δ be set to 0.1 experimentally. They also assumed that the cross traffic obeys the fluid model, and that all packet pairs in a packet train operate in the same queuing region.

When a packet train operates in a JQR, the inter-departure time of a packet pair is regarded as being fully filled with cross traffic. As a result, the cross traffic rate, CT_{rate}^j, with respect to the j-th packet train can be derived as

$$CT_{rate}^j = \frac{\sum_{i=1}^{P_{length}} (\Delta_{out}^i \times TC - L)|_{i\text{-th packet pair operates in a JQR}}}{\sum_{i=1}^{P_{length}} \Delta_{in}^j}, \tag{8}$$

where TC denotes the tight-link's capacity and the constant value, L, denotes the probing packet size. Since IGI is assumed to operate in a single-hop environment, the capacity (BC) of the bottleneck link is equal to that of the tight link. However, in a multi-hop environment, it is known that $BC \leq TC$. Therefore, the available bandwidth, $Avbw$, after the j-th packet train is probed is estimated as

$$Avbw = BC - CT_{rate}^j. \tag{9}$$

However, if the threshold δ in Eq. (7) cannot be accurately set, then the queuing region in which a packet train operates will be wrongly determined, leading to under-estimation of the available bandwidth. A scenario is depicted in Fig. 2, where a decreasing gap that is a JQR is wrongly determined as being a DQR (disjoint queuing region) due to the assumption that the fluid traffic model is used. In addition, if IGI is applied in a multi-hop environment, then the cross traffic rate in Eq. (8) will be under-estimated (because BC is used in place of TC), and the available bandwidth will be over-estimated accordingly. These estimation errors are proportional to the increasing difference between the tight-link's capacity and the bottleneck-link's capacity. These two problems constitute the main weaknesses of IGI.
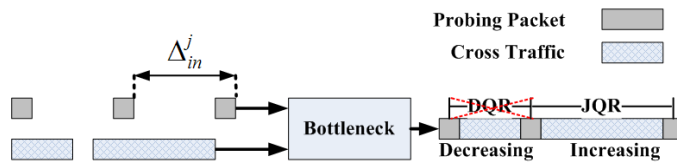
Fig. 2. An error in PGM, where the probing rate is higher than the available bandwidth, and the cross traffic rate decreases progressively during measurement. The decreasing gap is, in fact, a JQR, but IGI erroneously determines it to be a DQR.

III. PROPOSED METHOD

The concepts behind our method are briefly described as follows. Based on the principle of active probing, we have developed a method for repeatedly sending a packet train at a fixed input probing rate into a network such that the relationship between the input probing rate and output probing rate can be measured to infer the available bandwidth. The output probing rate is changed by the input probing rate because the sent packet train may be affected by cross traffic in that the time interval between a packet pair is either compressed or expanded. Here, a probing packet train is composed of several packet pairs, and the time interval between a packet pair is called the "probing gap." In other words, the "input probing gap" is defined as the inter-departure time of a packet pair sent from the sender, while the "output probing gap" is defined as the inter-arrival time of a packet pair reaching the receiver.

In Sec. III-A, a strategy for queuing delay propagation model (QDPM)-based queuing region determination is presented. It is used to classify the output gaps of a packet train at the receiver side into two types: joint queuing regions (JQRs) and disjoint queuing regions (DQRs). In addition, the queuing delay is updated once a packet pair has been processed by the router. Due to the bursty behavior of cross traffic on the Internet, the estimation error in queuing region determination is discussed in Sec. III-B. Since the initial queuing delay is unknown, its value is discussed in Sec. III-C. Then, in Sec. III-D, we exploit the types of queuing regions and the magnitude relationship between the total output gaps accumulated in JQRs and the total input gaps to investigate the relationship between the probing rate and available bandwidth. By sending a packet train with a certain input probing rate, we can adjust the next input probing rate by means of binary search, as will be described in Sec. III-E. During the period when packet trains are repeatedly sent, the probing rate can be gradually adjusted to approximate the available bandwidth.

There are two major characteristics of our method: (1) it can work without assuming the use of a fluid traffic model; (2) because it does not rely on the use of the bottleneck link's capacity to indicate the relationship between the probing rate and available bandwidth, our method can work in a multi-hop environment.

A. Queuing Delay Propagation Model (QDPM)-based Queuing Region Determination

The queuing region (QR) of a packet pair determines the relationship between a packet pair and the captured cross traffic. QRs can be classified into two types: joint queuing regions (JQRs) and disjoint queuing regions (DQRs). More specifically, a JQR is strictly defined as the situation where the time interval between a packet pair is fully filled with cross traffic. Based on these observations, in the next section, we will present a strategy for queuing region determination.

1) Queuing Region Determination: Let PP^i ($1 \leq i \leq P_{length}$), which is composed of consecutive probing packets P^{i-1} and P^i, denote the i-th packet pair in the j-th packet train, whose inter-departure time (the input gap between a packet pair) is Δ_{in}^j. Let QR^i denote the queuing region of PP^i. If PP^i is defined as operating in a JQR, then the bottleneck router does not finish three tasks before the arrival of P^i: processing the queued traffic (let Q^{i-1} denote the queued traffic when P^{i-1} arrives at the router), processing P^{i-1} (let L be the constant packet size), and processing the cross traffic inserted between this packet pair PP^i (let CT^i denote the amount of cross traffic inserted between PP^i). They can be related to each other as

$$(\frac{Q^{i-1} + L + CT^i}{TC}) > \Delta_{in}^j, \ \ \text{if} \ QR^i \text{ is a JQR}, \tag{10}$$

where TC denotes the capacity of a tight-link. Based on the definition of a JQR, the inter-arrival time of a packet pair PP^i measured at the receiver side is $\frac{L+CT^i}{TC}$, which is the output gap, Δ_{out}^i. In addition, let Q^{i-1}/TC denoted as D^{i-1} be the queuing delay that accumulates before packet P^{i-1}. Thus, Eq. (10) can be rewritten as

$$\Delta_{out}^i > (\Delta_{in}^j - D^{i-1}), \ \ \text{if} \ QR^i \text{ is a JQR}. \tag{11}$$

As shown in Eq. (11), we define what can be derived if a packet pair is a JQR. In order to determine the queuing region type of a packet pair, what the receiver needs based on Eq. (11) is the input and output gaps, and the queuing delay. In practice, when Δ_{out}^i is larger than $\Delta_{in}^j - D^{i-1}$, this implies that we can only know that this packet-pair captures a certain amount of cross traffic; however, packet pair PP^i cannot be determined as a JQR because the captured cross traffic is not guaranteed to completely fill this gap. If $\Delta_{out}^i > (\Delta_{in}^j - D^{i-1})$ and room exists within a packet pair, then the output gap is a DQR but is erroneously determined to be a JQR. This phenomenon is called an "estimation error," which will be described in more detail in Sec. III-B. When estimation errors can be completely eliminated, the receiver can use the following rule for queuing region determination:

$$QR^i \text{ is JQR, if } \Delta_{out}^i > (\Delta_{in}^j - D^{i-1}). \tag{12}$$

On the other hand, because the queuing delay D^{i-1} cannot be observed from a single packet pair, the sending packet trains is adopted in this study.

2) Queuing Delay Propagation: Once the queuing region of a packet pair PP^i has been determined based on Eq. (12), the queuing delay D^i that accumulates after PP^i needs to be calculated so that the next queuing region can be determined. Recall that the queuing delay is calculated using Eqs. (3) and (5) for a single-hop environment and multi-hop environment, respectively. If a packet pair, PP^i, operates in a JQR, the amount of traffic that queues before packet P^{i-1}, denoted as Q^{i-1}, will be propagated to probing packet P^i such that the total amount of traffic that queues before packet P^i, denoted as Q^i, will be composed of Q^{i-1}, the size of P^i, and the amount of cross traffic that arrives between P^{i-1} and P^i. Therefore, depending on whether PP^i operates in a JQR or not, the queuing delay that accumulates in front of packet P^i can be derived as

$$D^i = \begin{cases} D^{i-1} + \Delta^i_{out} - \Delta^j_{in}, \text{ if } QR^i \text{ is JQR} \\ max(0, \Delta^i_{out} - \Delta^j_{in}), \text{ otherwise,} \end{cases} \tag{13}$$

where $D^i = Q^i/TC$. As a result, if the procedures shown in Eqs. (12) and (13) are iteratively performed, queuing region determination and queuing delay propagation can be accomplished. In addition, it is also obvious that the queuing delay and the relationship between probing gaps (i.e., Δ^j_{in} and Δ^i_{out}) are two key factors in this study. However, it should be noted that D^0, the "initial queuing delay," is the queuing delay in front of the first probing packet in a packet train and is still unknown. In Sec. III-C, we shall explain how D^0 can be determined.

3) Unequal Weighted Output Gaps: Analogous to PRM-based methods, our method exploits a one-way delay-type mechanism to analyze the relationship between the available bandwidth and probing rate. The main difference between our method and other PRM-based methods is that it exploits the magnitudes of queuing delays while the others exploit the variation of queuing delays (i.e., increasing trend) in a probing train. In other words, our method *locally* exploits the magnitude of the queuing delay for each packet pair that operates in a JQR instead of relying on the *global* one-way delay increasing trend. In addition, there are three types of magnitude relationships between the input and output gaps in our approach: decreasing, equal, and increasing. In the following, we will explain how they affect queuing region determination and queuing delay propagation. It should be noted that in the following discussion, we assume that estimation errors can be alleviated (as will be explained in Sec.III-B).

a) Decreasing Output Gap ($\Delta^i_{out} < \Delta^j_{in}$): When a probing packet arrives at the router, it is either queued or sent immediately. If the probing packet P^{i-1} is queued due to previous un-processed aggregated traffic, the output gap between P^{i-1} and the subsequent probing packet P^i will decrease. Two situations may occur in the output gap of the packet pair PP^i. In the first one, no or little cross traffic is inserted between the probing packet pair,

as shown in Fig. 3(a), such that no gap remains. Under this circumstance, this packet pair operates in a DQR, and

its output gap is equal to $\Delta_{in}^{j} - D^{i-1}$. In the second case, cross traffic completely fills the gap between the packet

pair such that the output gap is larger than $\Delta_{in}^{j} - D^{i-1}$ but is still smaller than the input gap, as shown in Fig.

3(b). Under this circumstance, this packet pair operates in a JQR. Based on the condition that $\Delta_{out}^{i} < \Delta_{in}^{j}$ holds,
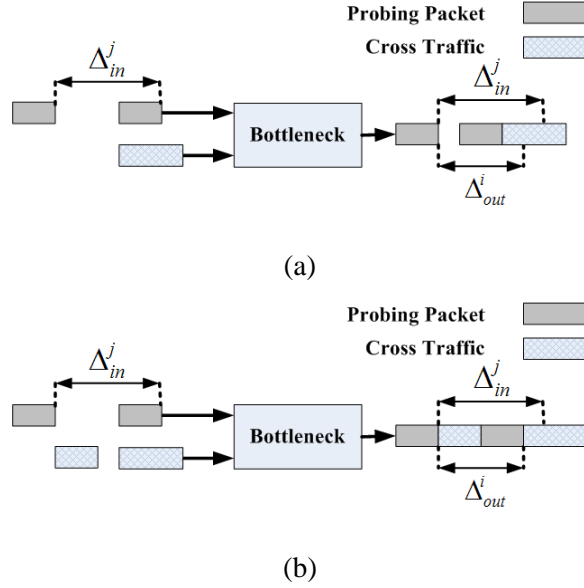

(a)

(b)

Fig. 3. Decreasing output gap (the probing gap is decreased by the queuing delay of the preceding probing packet): (a) the output gap is a DQR; (b) the output gap is a JQR.

Eqs. (12) and (13) for queuing region determination and delay propagation can be rewritten, respectively, as

$$QR^i \text{ is } \begin{cases} \text{JQR, if } \Delta_{out}^{i} > (\Delta_{in}^{j} - D^{i-1}) \\ \text{DQR, otherwise} \end{cases} \tag{14}$$

and

$$D^i = \begin{cases} D^{i-1} + \Delta_{out}^{i} - \Delta_{in}^{j}, \text{ if } QR^i \text{ is JQR} \\ 0, \text{ otherwise,} \end{cases} \tag{15}$$

where $D^i < D^{i-1}$.

b) Equal or Increasing Output Gap ($\Delta_{out}^{i} \geq \Delta_{in}^{j}$): Similarly, an equal output gap and an increased output gap

are illustrated in Figs. 4 (a) and (b), respectively. According to Eq. (12) and $\Delta_{out}^{i} \geq \Delta_{in}^{j}$, the output gap operates

in a JQR if the current queuing delay is larger than zero, i.e.,

$$QR^i \text{ is } \begin{cases} \text{JQR, if } D^{i-1} > 0 \\ \text{DQR, otherwise.} \end{cases} \tag{16}$$

Similarly, Eq. (13) for queuing delay propagation can be rewritten as

$$D^i = \begin{cases} D^{i-1} + \Delta_{out}^i - \Delta_{in}^j, & \text{if } QR^i \text{ is JQR} \\ \Delta_{out}^i - \Delta_{in}^j, & \text{otherwise,} \end{cases} \tag{17}$$

where $D^i \geq D^{i-1}$. When the output gap is larger than or equal to the input gap, our method is degenerated into an OWD increasing trend mechanism.
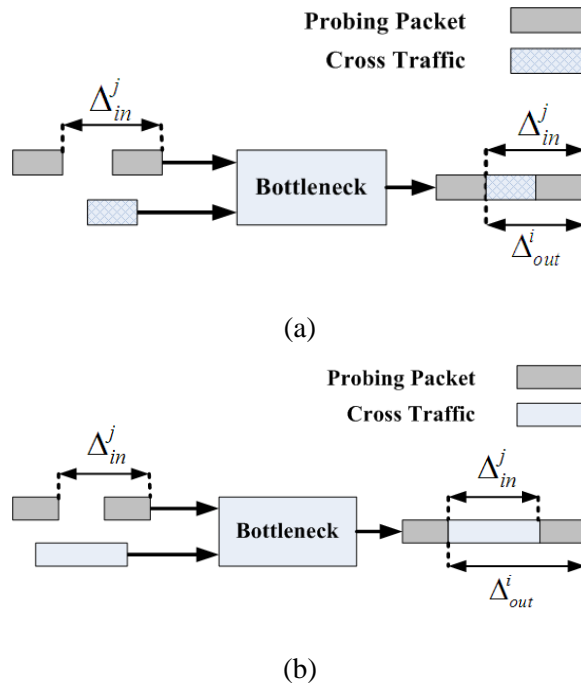

(a)

(b)

Fig. 4. Equal and increased output gaps (the input gap remains unchanged or increases due to the insertion of cross traffic): (a) the output gap is equal to the input gap; (b) the output gap is larger than the input gap.

Finally, the above derivations show that the phenomena of decreasing and increasing output gaps will last for a period and will not occur in an interleaving manner if the bursty behavior of the major traffic on the Internet, i.e., TCP traffic, is considered.

B. Estimation Error

In the previous section, we explained how the different types of queuing regions can be determined. However, a DQR may be falsely determined to be a JQR, which is called an "estimation error" in this study. In this case, the queuing region of a packet pair satisfying the relationship shown in Eq. (12) will be determined to be a JQR even when there is, in fact, some room left in the queuing region, which is not compeletely filled with cross traffic. This phenomenon is caused by the bursty behavior of cross traffic, which behaves like the major traffic on the Internet. In addition, the room remaining in the output gap is generally called "probing noise." Actually, estimation errors

constitute a critical problem affecting the accuracy of our method. In this section, the impact of estimation errors on the accuracy of our method will be investigated based on two different relationships between input gaps and output gaps, as described in Sec. III-A.3. Since the bursty behavior of TCP traffic prevents fragmentary estimation errors from occurring, we will not discuss them in this paper.

In the first case, the output gap of a packet pair PP^k, which is a reduced gap and is contaminated by probing noise, is assumed to satisfy Eq. (14). Under these circumstances, the queuing region QR^k of PP^k is determined to be a JQR, but it actually operates in a DQR. As a result, the queuing delay D^k of PP^k will satisfy the relationship $D^k < D^{k-1}$, according to Eq. (15). If probing noise continues to exist in the sequence of decreasing output gaps, then the queuing delays of subsequent probing packet pairs will also form a decreasing sequence. Since the queuing delay cannot be negative, the probing noise can be finally eliminated until the queuing delay reaches zero.

In the second case, the output gap of a packet pair PP^k, which is an equal or increasing gap and is contaminated by probing noise, is assumed to satisfy Eq. (16). Under these circumstances, the queuing region QR^k of PP^k is determined to be a JQR, but it actualy operates in a DQR. As a result, the queuing delay D^k of PP^k will satisfy the relationship $D^k \geq D^{k-1}$, according to Eq. (17). If probing noise continues to exist in the sequence of increasing output gaps, then the queuing delays of subsequent probing packet pairs will also form an increasing sequence. Since the increased queuing delay will reduce subsequent output gaps, probing noise can be finally eliminated until the bottleneck gap appears [2]; i.e., two packets can be connected without any space between them.

From the above discussions, it is clear that probing noises can be eliminated after a few packets have been probed. In order to quickly reduce the effect of probing noises, we will examine the key factor that can be used to achieve this goal. As described previously, the output gap, which is originally equal to the input gap, plays the key role. Therefore, we find that the size of the input gap is closely related to the amount of time that is required to eliminate probing noises. Intuitively, the shorter the input gap is, the faster the probing noises will disappear. Thus, the size of the probing packets has to be also reduced in order to maintain the same probing rate, $\frac{L}{\Delta_{in}^j}$. Under these circumstances, a shorter packet train is used here for available bandwidth estimation. However, a shorter packet train can only provide short-term measurements. In order to get a long-term measurement, a longer probing train is needed.

C. Determining the Initial Queuing Delay (D^0)

As described in Sec. III-A, the queuing delay and cross traffic play key roles in determining the magnitude relationship between the input gap Δ_{in}^j of the j-th packet train and the output gap Δ_{out}^i of the i-th packet pair.

Both of them are exploited here to determine the initial queuing delay. Our method only needs to trace the output gaps of a packet train once for initial queuing delay determination. We will investigate this issue based on two cases.

First, we will consider the case where the output gap is smaller than the input gap, i.e., $\Delta_{out}^i < \Delta_{in}^j$, as described in Sec. III-A.3.a. This means that the first output gap is decreased to absorb the initial queuing delay. The size of the first output gap depends on two factors: the queuing delay and cross traffic. If there is no cross traffic, or if the amount of inserted cross traffic is not large enough to expand the first output gap, then the difference $\Delta_{in}^j - \Delta_{out}^1$ is equal to the initial queuing delay D^0. On the other hand, if D^0 is too large to be absorbed in the first output gap, i.e., $D^0 > \Delta_{in}^j - \Delta_{out}^1$, then the subsequent output gaps will be gradually decreased to absorb the remaining queuing delay. Propagation of the queuing delay will continue, and a decreasing sequence of queuing delays, $D^0 > D^1 > \cdots > D^{k-1}$, will be generated until $D^{k-1} < D^k$ that is caused by the inserted cross traffic is satisfied. This means that the initial queuing delay will be completely exhausted. Since D^0 is unknown when probing begins, it is set to zero initially during queuing delay propagation, and can be calculated and found to be the absolute value of D^{k-1}, $|D^{k-1}|$.

In the second case that we will consider, the first output gap is larger than or equal to the input gap, i.e., $\Delta_{out}^1 \geq \Delta_{in}^j$, as described in Sec. III-A.3.b. In this situation, we cannot be sure if the initial queuing delay will be completely absorbed in the first output gap or if it does not exist initially. However, we can infer the queuing delay D^1 of the second packet by Eq. (17) and use it as though it were the initial queuing delay, though we will lose the aggregated traffic captured in the first output gap. This phenomenon is regarded as a kind of noise that may slightly affect the "captured traffic ratio" determination (which will be discussed in the next section). However, the impact of this type of a noise on the accuracy of available bandwidth estimation may, in fact, be negligible when compared with the impact of probing noise.

D. Relationship between the Probing Rate and Available Bandwidth?

After the queuing regions and queuing delays of a packet train have been determined, the so-called "captured traffic ratio (CTR)" can be calculated to determine the relationship between the probing rate and available bandwidth. Then, the next probing rate can be adjusted through binary search.

1) Captured Traffic Ratio (CTR): When a single packet pair is considered, the relationship between the probing rate (R) and available bandwidth ($Avbw$) can be expressed as

$$R > Avbw \text{ iff } \frac{L}{\Delta_{in}} > (TC - \frac{CT}{\Delta_{in}}), \tag{18}$$

where $R = \frac{L}{\Delta_{in}}$ denotes the probing rate of a packet pair, $\frac{CT}{\Delta_{in}}$ denotes the cross traffic rate captured by the packet pair, and $TC - \frac{CT}{\Delta_{in}}$ denotes $Avbw$. When a packet train is considered, Eq. (18) can be rewritten for all packet pairs of the j-th probing packet train as

$$R^j > Avbw \text{ iff } \sum_{i=1}^{P_{length}} (CT^i + L) > P_{length} \times TC \times \Delta_{in}^j. \tag{19}$$

The cross traffic in Eq. (19) can be further classified into two types according to the kind of queuing region in which a packet pair operates. By distinguishing between different queuing regions, Eq. (19) can be rewritten as

$$R^j > Avbw \text{ iff }$$

$$\frac{\sum_{i=1}^{P_{length}} (CT^i + L)|_{QR^i \text{ is JQR}} + \sum_{i=1}^{P_{length}} (CT^i + L)|_{QR^i \text{ is DQR}}}{P_{length} \times TC \times \Delta_{in}^j} > 1. \tag{20}$$

However, no clue can be used to estimate the amount of cross traffic in a DQR. Consequently, only the cross traffic, which is captured in JQRs, can be exploited to determine the relationship between the probing rate and available bandwidth. By taking the estimated cross traffic into consideration, we can rewrite Eq. (20) as

$$R^j > Avbw, \text{ if } \frac{\sum_{i=1}^{P_{length}} (CT^i + L)|_{QR^i \text{ is JQR}}}{P_{length} \times TC \times \Delta_{in}^j} > 1. \tag{21}$$

Substituting $\Delta_{out}^i = \frac{CT^i + L}{TC}$ into Eq. (21), we have

$$R^j > Avbw, \text{ if } \frac{\sum_{i=1}^{P_{length}} \Delta_{out}^i|_{QR^i \text{ is JQR}}}{P_{length} \times \Delta_{in}^j} = \text{CTR} > 1, \tag{22}$$

where CTR denotes the "captured traffic ratio," which measures the total output gaps accumulated in JQRs per the total number of input gaps.

We should note that the number of output gaps accumulated in DQRs is related to the probing noise, as described in Sec. III-B. Let ϵ denote the probing noise ratio, which plays a role opposite to that of CTR in our estimation of the available bandwidth. In Sec. IV, we will also discuss how ϵ can be detected.

Finally, by exploiting the derived CTR and by taking probing noises into consideration, we can specify the relationship between the probing rate and available bandwidth by revising Eq. (22) and obtaining

$$R^j > Avbw, \text{ if } CTR > 1,$$
$$R^j < Avbw, \text{ if } CTR < 1 - \epsilon. \tag{23}$$

In Eq. (23), if CTR falls within the interval $[1 - \epsilon \quad 1]$, then the sender must use a higher probing rate to alleviate the effect of probing noises. This problem will be discussed in the next section.

E. Probing Rate Adjustment

According to Eq. (23), the relationship between the probing rate of the j-th packet train and the available bandwidth can be determined. In order to get a more accurate estimate, binary search [8] is adopted to iteratively approximate the available bandwidth. Due to the bursty characteristic of TCP, the available bandwidth is not actually constant, so only an approximate estimate of the available bandwidth can be obtained.

Given a probing rate R^j of the j-th packet train and an available bandwidth *Avbw*, the next probing rate and its boundaries (R_{min} and R_{max}) can be determined as follows:

$$
\begin{aligned}
R_{min} = R^j, \ \ \text{if} \ R^j > Avbw, \\
R_{max} = R^j, \ \ \text{if} \ R^j < Avbw, \\
R^{j+1} = (R_{min} + R_{max})/2,
\end{aligned}
\tag{24}
$$

where R_{min} denotes the upper bound of $Avbw$ and R_{max} denotes the lower bound of $Avbw$. Although no guideline is available for setting the initial values of R_{min} and R_{max}, we recommend that R_{min} be set to the upper bound of the available bandwidth, which is equal to the capacity of the bottleneck link, and that R_{max} be set to the lower bound of the available bandwidth, which is, ideally, zero. On the other hand, if $1 - \epsilon \leq CTR \leq 1$, then both R_{min} and R_{max} should be kept un-changed, and the next probing rate R^{j+1} should be set to a higher value, $\frac{R_{min}+R^j}{2}$. The above probing rate adjustment procedure stops if $|R_{min} - R_{max}| < \omega$ holds such that the degree of fluctuation of the available bandwidth is bound to ω, which is called the "estimation resolution." We will explain how ω can be set in Sec. IV. When the stop condition is satisfied, R_{max} is adopted as the estimated available bandwidth. In addition, R_{min} is adopted as the next initial probing rate when the available bandwidth procedure restarts.

So far, it can be seen that the proposed method tries to find the available bandwidth by pouring traffic into the network. Once the buffer of the router overflows, the incoming data will be dropped, leading to packet loss. Here, we assume that packet loss is caused by congestion, which only occurs in a wired environment. Under this circumstance, if the receiver detects probing packet loss, then the sender has to adjust the new probing rate using the AIMD mechanism [6]. However, when the probing rate is reduced to be less than R_{max}, this adjustment is not helpful for enabling the probing rate to converge to the available bandwidth (as will be discussed in the next section). Thus, we propose reducing the next probing rate to $\frac{R_{max}+R^j}{2}$ instead of $\frac{R^j}{2}$. Since the length (200 packets) of our probing packet train, when compared with TCP window sizes (the maximum size is 64K packets), is quite small, our probing rate adjustment even without obeying the AIMD mechanism will not cause significant unfairness.

IV. ANALYSIS: PROBING NOISE RATIO (ϵ) VS. ESTIMATION RESOLUTION (ω)

In this section, we shall investigate the relationship between the probing noise ratio (ϵ) and the estimation resolution (ω). Since probing noise, as described in Sec. III-B, cannot be detected in practice, we propose to quantify it in an ideal case when the probing rate is equal to the available bandwidth. This ideal case is adopted for two reasons: (1) no useful information can be obtained from the case in which the probing rate is lower than the available bandwidth; (2) since the true available bandwidth varies dynamically, the ratio of probing noise can be detected in the worst case when the probing rate is equal to the available bandwidth, which means that $CTR = 1$ (as opposed to Eq. (22)). Suppose that the maximum and minimum cross traffic rates are $\frac{CT}{\Delta_{in}^j} + \tau_1$ and $\frac{CT}{\Delta_{in}^j} - \tau_2$, respectively. In order to simplify the analysis, we assume that $\tau_1 = \tau_2 = \tau$, and that the cross traffic rates are restricted to only two values, $\frac{CT}{\Delta_{in}^j} + \tau$ and $\frac{CT}{\Delta_{in}^j} - \tau$, so that analytic results for the extreme case can be obtained. Under these circumstances, if a packet pair captures the cross traffic with a rate of $\frac{CT}{\Delta_{in}^j} + \tau$, then its queuing region will be filled and expanded by the captured cross traffic and determined to be a JQR. On the other hand, the queuing region of a packet pair, which captures cross traffic with a rate of $\frac{CT}{\Delta_{in}^j} - \tau$, is a DQR and may become a JQR if this packet pair can receive the propagated queuing delay of the preceding packet pairs.

In the situation where the probing rate is equal to the available bandwidth, it is reasonable to assume that the numbers of packet pairs, which capture cross traffics with two different rates, are the same and are set to M. In addition, let K ($\leq M$) denote the number of packet pairs that capture cross traffic with a rate of $\frac{CT}{\Delta_{in}^j} - \tau$ and receive sufficient queuing delays such that their queuing regions become JQRs. The amount of cross traffic, $(\frac{CT}{\Delta_{in}^j} + \tau)\Delta_{in}^j$, captured by the M packet pairs and the amount of cross traffic, $(\frac{CT}{\Delta_{in}^j} - \tau)\Delta_{in}^j$, captured by the K packets are, respectively, substituted for CT^i of Eq. (21), we have the following derivation:

$$CTR = \frac{M \times (CT + \tau \times \Delta_{in}^j + L)}{2M \times TC \times \Delta_{in}^j} + \frac{K \times (CT - \tau \times \Delta_{in}^j + L)}{2M \times TC \times \Delta_{in}^j}. \tag{25}$$

Since the probing rate is assumed to be equal to the available bandwidth, we have $TC - \frac{CT}{\Delta_{in}^j} = \frac{L}{\Delta_{in}^j}$. Substituting $TC \times \Delta_{in}^j$ into $CT + L$ of Eq. (25), we can express CTR as

$$CTR = \frac{M + K}{2M} + \frac{(M - K) \times \tau}{2M \times TC}. \tag{26}$$

Ideally, the ratio of probing errors, ϵ, that originated from bursty cross traffic (which also implies fluctuation of the available bandwidth) will be derived as $1 - CTR$, i.e.,

$$\epsilon = \frac{(M - K) \times (TC - \tau)}{2M \times TC}. \tag{27}$$

In Eq. (27), the maximum value of ϵ (which can result in the maximum number of queuing regions determined to be DQRs) is found if $K = 0$. Substituting $K = 0$ into Eq. (27), we can derive ϵ as

$$\epsilon = \frac{TC - \tau}{2 \times TC}. \tag{28}$$

Since the tight-link's capacity, TC, is not known, the bottleneck-link's capacity, BC, replaces TC in our implementation. In this case, the detected ϵ is larger than it should be.

In order to reduce the number of probing errors, the sender needs to use a higher probing rate, i.e., the additional rate ω, to exhaust the unused bandwidth, such that the aggregated traffic will fill the gaps between packet pairs. Therefore, the estimation resolution, ω, is used in place of TC, and $K = M$ is set to obtain the maximum compensation of the second term on the right-hand side in Eq. (25):

$$\frac{M \times (CT + L - \tau \times \Delta_{in}^{j})}{2M \times \omega \times \Delta_{in}^{j}} \leq 1. \tag{29}$$

Again, substituting $TC \times \Delta_{in}^{j}$ into $CT + L$ of Eq. (29), we have

$$\omega \geq \frac{TC - \tau}{2}. \tag{30}$$

Given Eqs. (28) and (30), the relationship between ω and ϵ can be derived as

$$\omega \geq TC \times \epsilon. \tag{31}$$

The estimation resolution, ω, plays a key role in the trade-offs among the estimation accuracy, convergence speed, and intrusiveness of the proposed method. More specifically, it can be found that a small value of ω can yield more accurate estimation results at the expense of increased probing time (i.e., intrusiveness). Due to Eq. (31), the minimum ω should be adjusted according to the degree of fluctuation of the available bandwidth, which is also indicated by ϵ.

V. SIMULATION RESULTS

In order to demonstrate the performance of our method, several simulations using ns2 [16] were conducted based on two different network models, shown in Figs. 5 and 6, respectively. The proposed method was also compared with PathChirp [21] and IGI [2] in terms of the accuracy and smoothness of available bandwidth estimation. PathChirp and IGI were selected because they are, respectively, typical examples of PRM- and PGM-based mechanisms. In this study, two different types of cross traffic, constant bit-rate (CBR) traffic and FTP traffic, were considered because CBR traffic is a kind of fluid model, and because FTP traffic, which exhibits bursty behavior, is the main type of
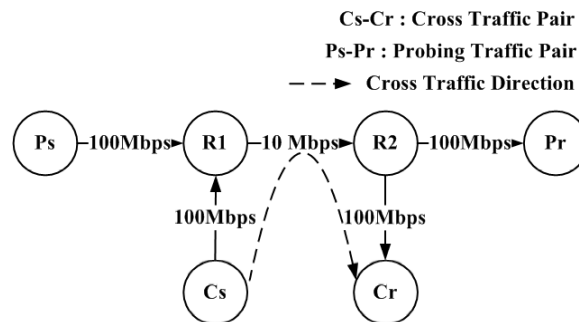
Fig. 5.   A single-hop model, where the bottleneck link is the same as the tight-link, and bottleneck bandwidth is set to 10Mbps.
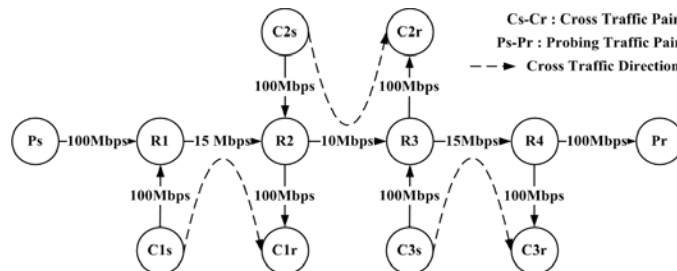

Fig. 6.   Multi-hop network model. The bottleneck link maybe not equal to the tight-link.

traffic on the Internet. The packet size for the CBR traffic was fixed at 1000 bytes. The maximum throughput of the FTP traffic was set to 1024 packets/flow.

In our simulations, the value of ω was initially set to 200 kbps, and its range could be dynamically changed according to the detected value of ϵ, as indicated in Eqs. (28) and (31). Here, the lower bound of ω was adopted as the estimation resolution. The probing rate was initially set to half of the bottleneck link's capacity, and its variation during available bandwidth measurement is plotted using dash-dot curves in the figures shown below. With our method, we adopted a probing train composed of 200 packets, each of which was 1000 bytes in size. For IGI, we adopted a packet train composed of 60 packets with a packet size of 700 bytes, as suggested in [2] so that the best results could be obtained.

A. Single-Hop Network Environment

The first network topology, as shown in Fig. 5, specifies a single-hop environment, where Ps and Pr denote, respectively, the sender and receiver in the end-to-end probing path, and Cs and Cr denote, respectively, the sender and receiver in the cross traffic transmission path.

The results of available bandwidth estimation obtained using our method, IGI, and PathChirp, and the true available bandwidth are plotted in Fig. 7 for comparison purpose, based on the assumption that the cross traffic is

composed of CBR traffic only, which also implies that the cross traffic rate is stable. It can be observed from Fig. 7 that our method and IGI are able to estimate the available bandwidth accurately and smoothly. On the other hand, PathChirp results in larger over-estimations when the network load is small, and yields improved but oscillatory estimations when the network load is large. Here, the network load is proportional to the cross traffic rate. The main reason for the poor performance of PathChirp is its limited ability to determine queuing regions.
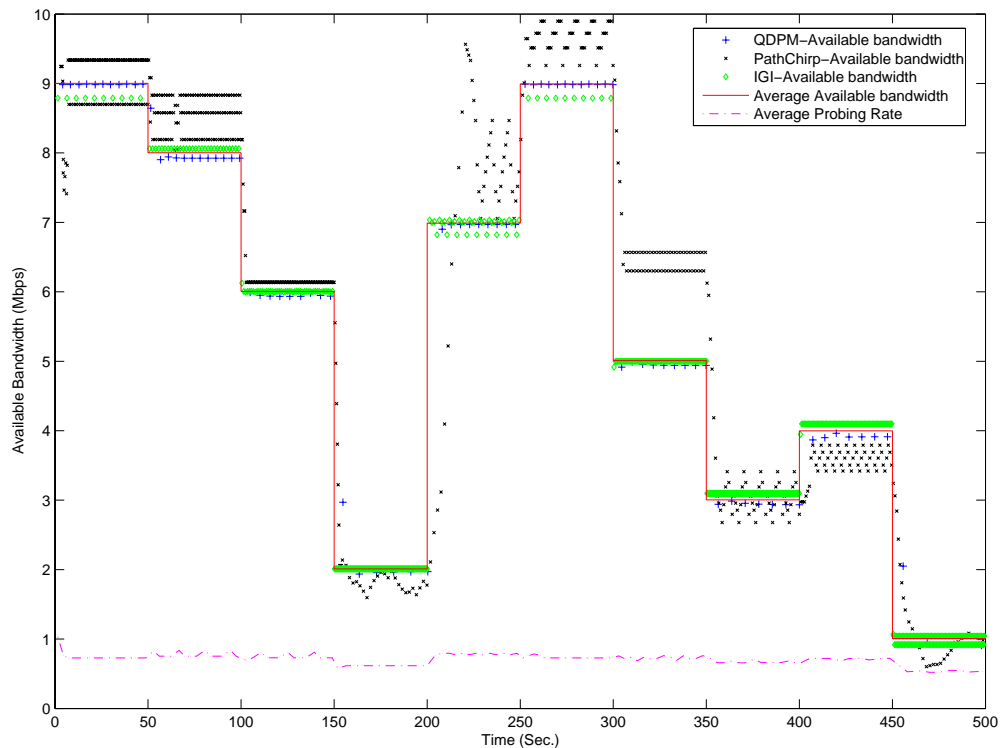

Fig. 7. Comparison of the available bandwidth estimation results obtained with the proposed method (QDPM), PathChirp, and IGI for the single-hop network model (Fig. 5) with CBR cross traffic only.

A simulation was also conducted based on the situation in which the cross traffic is composed of both CBR and FTP traffic. In this case, we added the first FTP flow at the beginning of network transmission and added the second FTP flow from Cs to Cr at the 250th second. Again, the estimation results are plotted in Fig. 8 for comparison purposes. It can be observed from Fig. 8 that our method is able to stably detect the true available bandwidth with only slight over-estimations when the cross traffic rate is low. These slight over-estimations are mainly due to two factors: (i) the effect of probing noise; and (ii) the bursty behavior of FTP traffic, which causes the estimated available bandwidth to be transient instead of smooth. On the other hand, we find that PathChirp generates over-estimations when the cross traffic rate is low and yields improved but oscillatory estimations when

the cross traffic rate is high, while IGI produces mostly under-estimations and large deviations due to erroneous turning point detection. Again, the main reason for the inaccuracy of both PathChirp and IGI is their assumption that the fluid cross traffic model is used. When non-fluid traffic like FTP is encountered, our method obtains more accurate estimates than either PathChirp or IGI.
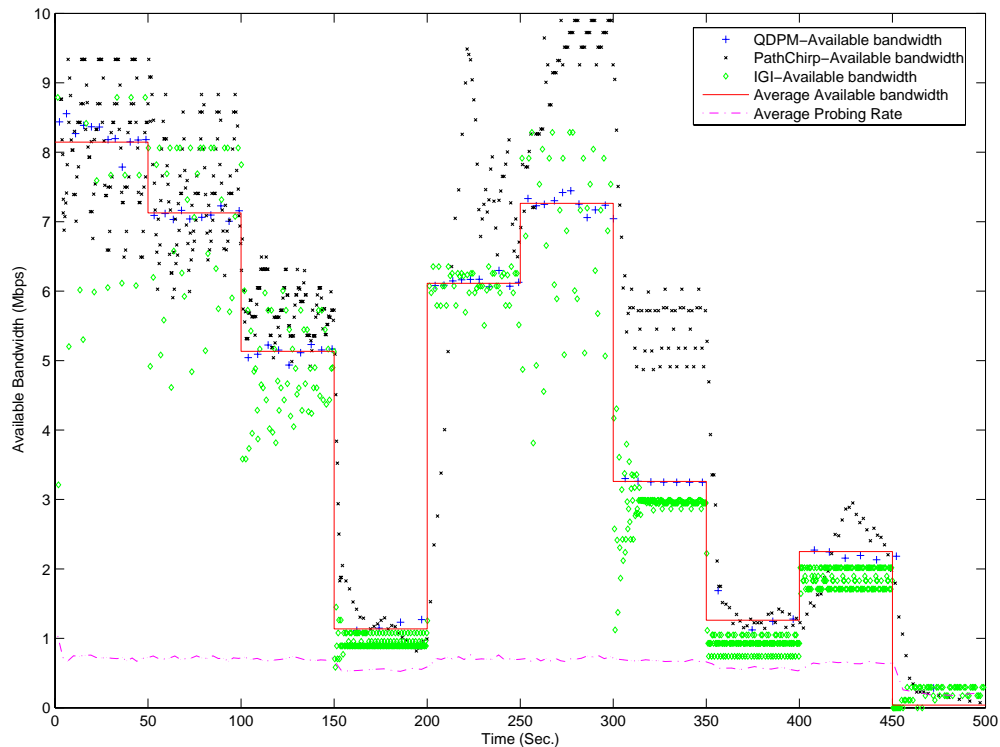

Fig. 8. Comparison of the available bandwidth estimation results obtained with the proposed method (QDPM), PathChirp, and IGI for the single-hop network model (Fig. 5), where the cross traffic is composed of both CBR and FTP traffic.

B. Multi-hop Network Environment

The performance of our method, IGI, and PathChirp was verified and compared using a multi-hop network topology, as shown in Fig. 6. The results revealed the most important advantage of our method. It should be noted that the available bandwidth of this end-to-end path is the minimum un-used bandwidth among the three links. In the network setting, the bandwidth of the first link (R1-R2) was set to 15 Mbps, the bandwidth of the second link (R2-R3) was set to 10 Mbps, and the bandwidth of the third link (R3-R4) was set to 15 Mbps. The bottleneck was initially located at the bottleneck link (R2-R3) and could be shifted to other links if the cross traffic rate in each link was changed. The initial cross traffic rate in each link was 3 Mbps.

In this simulation, two bottleneck shifting scenarios were studied to verify the performance. First, the bottleneck was shifted to the link in front of the bottleneck link. This scenario could be achieved by increasing the cross traffic rate of link R1-R2 with an increasing ratio of 2 Mbps per 50 seconds until link R1-R2 finally became the bottleneck. In the second scenario, the bottleneck was shifted from link R1-R2 to link R3-R4. This could be achieved by increasing the cross traffic rate of link R3-R4 with an increasing ratio of 4 Mbps per 50 seconds until the bottleneck was finally transferred to R3-R4. In addition, it should be noted that the bottleneck was shifted from the second link to the first link at the 200th second, and was shifted from the first link to the third link at the 350th second.

In Figs. 9 and 10, the results for the estimated available bandwidth obtained with our method, PathChirp, and IGI, and the true available bandwidth are plotted for the purpose of comparison. The results shown in Fig. 9 were obtained when the cross traffic was composed of CBR flows only. It can be observed that our method was able to approximate the actual available bandwidth with only slight over-estimation. PathChirp yielded rather inaccurate estimations no matter whether the cross traffic rate was high or low. Meanwhile, we find that IGI only estimated the available bandwidth correctly when the bottleneck was exactly located at the bottleneck link. Therefore, the threshold for turning point determination, as indicated in Eq. (7), is a decisive factor affecting the performance of IGI. In summary, the major weakness of both PathChirp and IGI revealed in this simulation is that they tend to erroneously detect OWD increasing trend or obtain an erroneous turning point.

The estimation results shown in Fig. 10 were obtained when the cross traffic was composed of both CBR and FTP traffic. The bursty behavior of TCP flows could be simulated by first adding a FTP flow at the beginning of network transmission and adding a second FTP flow at the 200th second. It can be observed from Fig. 10 that both IGI and PathChirp yielded inaccurate and oscillatory estimations. Compared with PathChirp and IGI, our method can stably obtain estimations that are closer to the actual available bandwidth.

VI. Conclusion

Traditional transport protocols are unable to provide stable video transmission due to ignorance of the available bandwidth. Meanwhile, end-to-end available bandwidth estimation has been found to be helpful for congestion control of multimedia transmission. In this paper, we have proposed an accurate available bandwidth estimation method that is based on the queuing region propagation model (QDPM). The key to accurate bandwidth estimation is to exploit the relationships among queuing delays, input gaps, and output gaps so that the attribute of the queuing region in each packet pair can be determined. Then, the CTR, which is defined as the ratio of the total number
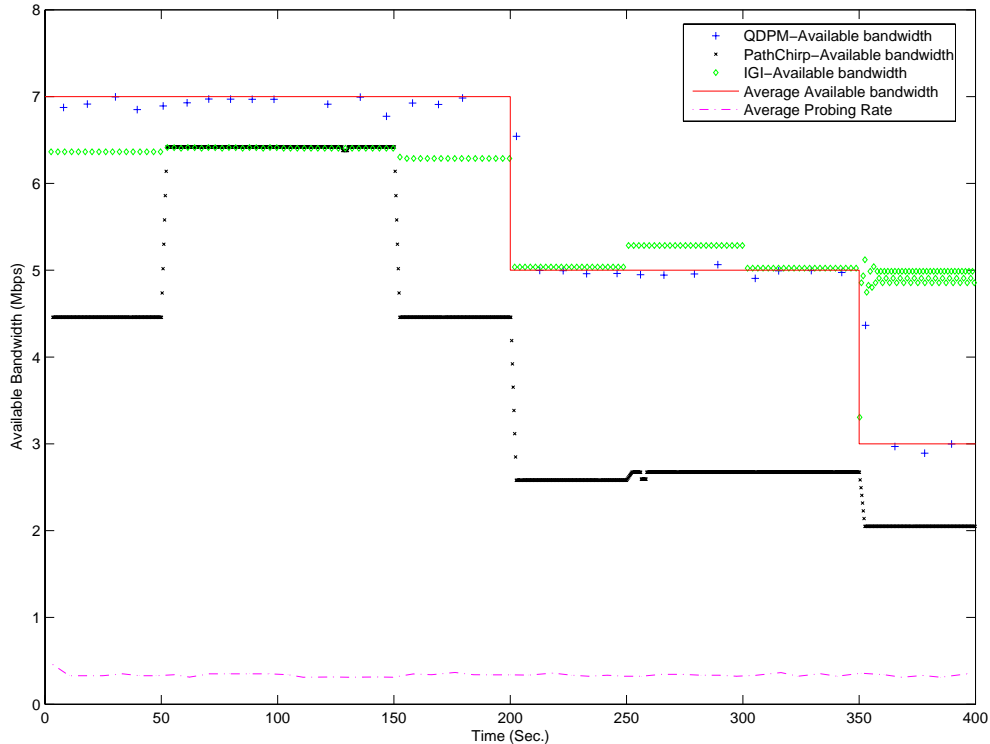
Fig. 9. Comparison of available bandwidth estimations obtained with the proposed method (QDPM), PathChirp, and IGI for the multi-hop network model (Fig. 6), where the cross traffic contains CBR traffic only.

of output gaps accumulated in JQRs to the total number of input gaps, can be used to specify the relationship between the probing rate and available bandwidth. A binary search-based probing rate adjustment mechanism has been proposed to approximate the available bandwidth with an error that is within the estimation resolution. The estimation resolution has been found to be closely related to the probing noise ratio. Thus, both of the parameters affecting the performance of our method can be automatically determined. Finally, several simulations and comparisons have been conducted to verify that smooth and accurate estimations can be obtained with the proposed QDPM method.

It is also important to point out that the rules of queuing-delay jitter calculation, as specified in Eqs. (3) and (5), are adopted in the proposed method, without the need for time-synchronization between the sender and receiver. Therefore, our method does not run the risk of encountering the clock offset problem. In addition, the clock skew problem is also negligible with our approach because the clock skew, which is on the order of a few nanoseconds [8], is much shorter than the time required to calculate the OWD jitter and is on the order of a few milliseconds. Finally, we will plan to further verify the proposed scheme via real networks.
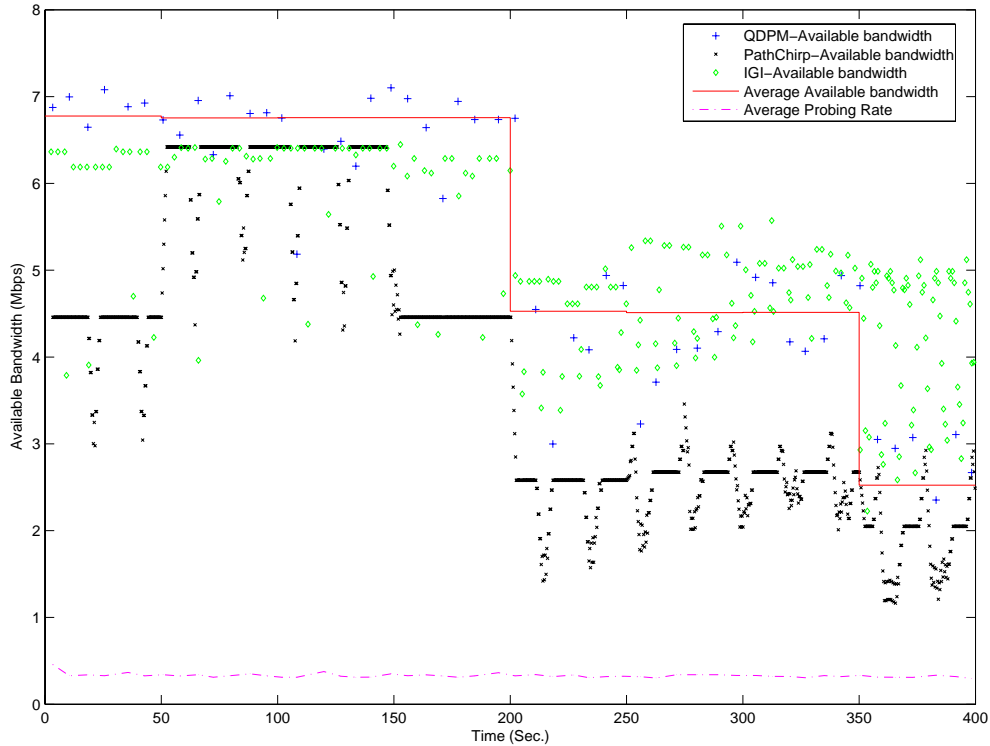
Fig. 10. Comparison of available bandwidth estimations obtained with the proposed method (QDPM), PathChirp, and IGI for the multiple-bottleneck network model (Fig. 6), where the cross traffic includes both CBR and FTP traffic.

REFERENCES

[1] D. Dutta, Y. Zhang, "An Early Bandwidth Notification (EBN) Architecture for Dynamic Bandwidth Environment," *Proc. IEEE Int. Conf. on Communications*, 2002.

[2] N. Hu and P. Steenkiste, "Evaluation and Characterization of Available Bandwidth Techniques," *IEEE Journal on Selected Areas in Communication: Special Issue in Internet and WWW Measurement, Mapping, and Modeling*, 2003.

[3] N. Hu and P. Steenkiste, "Improving TCP Startup Performance using Active Measurements: Algorithm and Evaluation," *Proceedings of the 11th IEEE International Conference on Network Protocols* , November 2003.

[4] Y. C. Huang, C. S. Lu, and H. K. Wu, "Reliable Available Bandwidth Estimation Based on Distinguishing Queuing Regions and Resolving False Estimations," *Proc. IEEE Global Telecommunications Conference (Globecom),* Dallas Texas, USA, 2004.

[5] Internet Measurement Conference, 2001∼2005.

[6] V. Jacobson, "Congestion Avoidance and Control," *Proceedings of ACM SIGCOMM*, pp.314-329, September 1988.

[7] M. Jain and C. Dovrolis, "End-to-End Available Bandwidth: Measurement Methodology, Dynamic, and Relation with TCP Throughput," *Proceedings of ACM SIGCOMM 2002*, 2002.

[8] M. Jain and C. Dovrolis, "Pathload: A Measurement Tool for End-to-End Available Bandwidth," *Proc. Passive and Active Measurements*, March 2002.

[9] M. Jain and C. Dovrolis, "Ten Fallacies and Pitfalls on End-to-End Available bandwidth Estimation," *Proceedings of the conference on Internet measurement conference*, October 2004.

[10] S. Keshav, "A Control-Theoretic Approach to Flow Control," *Proc. ACM SIGCOMM*, pp. 3-15, 1991.

[11] Z.G. Li, C. Zhu, N. Ling, X. K. Yang, G.N. Feng, S. Wu, and F.Pan, "A Unified Architecture for Real-Time Video-Coding Systems," *IEEE Trans. on Circuits and Systems for Video Technology*, 2003.

[12] J. Liu, B. Li, and Y. Q. Zhang, "Adaptive Video Multicast over the Internet," *IEEE Multimedia,* Vol. 10, No. 1, pp. 22-31, 2003.

[13] Q. Liu, and J. Hwang, "End-to-End Available Bandwidth Estimation and Time Measurement Adjustment for Multimedia QoS," *Proc. IEEE Int. Conf. on Multimedia and Expo*, 2003.

[14] M. Mathis and M. Allman, *A framework for Defining Empirical Bulk Transfer Capacity Metrics*, RFC 3148, July 2001.

[15] B. Melander, M. Bjorkman, and P. Gunningberg, "A New End-to-End Probing and Analysis Method for Estimating Bandwidth Bottlenecks," *Proc. Global Internet Symposium*, 2000.

[16] ns2 [Online]. http://www.isi.edu/nsnam/ns.

[17] J. Navratil, and R. L. Cottrell, "ABwE: A Practical Approach to Available Bandwidth Estimation," *Proc. Passive and Active Measurement Workshop*, 2003.

[18] V. Paxson, "End-to-end Routing Behavior in the Internet," *IEEE/ACM Transactions on Networking*, Vol. 5, No. 5, pp. 601-615, 1997.

[19] R. Puri, K. W. Lee, and K. Ramchandran, "An Integrated Source Transcoding and Congestion Control Paradigm for Video Streaming in the Internet," *IEEE Trans. on Multimedia*, 2001.

[20] V. J. Ribeiro, M. Coates, R. H. Riedi, S. Sarvotham, and R. G. Baraniuk, "Multifractal Cross Traffic Estimation," *Proc. of ITC specialist seminar on IP traffic Measurement*, 2000.

[21] V. J. Ribeiro, R. H. Riedi, R. G. Baraniuk, J. Navratil, and L. Cottrell, "PathChirp: Efficient Available Bandwidth Estimation for Network Paths," *Proc. Passive and Active Measurement Workshop*, 2003.

[22] V. J. Ribeiro, R. H. Riedi and R. G. Baraniuk, "Locating Available Bandwidth Bottlenecks," *Second International Workshop on Protocols for Fast Long-Distance Networks*, October 2004.

[23] J. Strauss, D. Katabi, and F. Kaashoek, "A Measurement Study of Available Bandwidth Estimation Tools," *Proceedings of the conference on Internet measurement Workshop*, pp. 27-29, October 2003.

[24] D. Wu, Y. T. Hou, and Y. Q. Zhang, "Transport Real-Time Video over the Internet: Challenges and Approaches," *Proceedings of the IEEE*, 2000.

[25] Y. Zhang, N. Duffield, V. Paxson, and S. Shenker, "On the Constancy of Internet Path Properties," Proceedings of *ACM SIGCOMM Internet Measurement Workshop*, Nov. 2001.